EURASIAN PHYSICAL TECHNICAL JOURNAL

2024, Volume 21, No.3 (49)

https://doi.org/10.31489/2024No3/54-62

Received: 22/03/2024 Revised: 03/07/2024 Accepted: 20/09/2024 Published online: 30/09/2024

Original Research Article

UDC 53.043, 546.05

SYNTHESIS AND CHARACTERIZATION OF HYDROXYAPATITE UNDER INFLUENCE OF ULTRAVIOLET RADIATION AND ULTRASONIC EXPOSURE

Mostovshchikov A.V.[1, 2], Grebnev M.E.[2], Rudmin M.A.[1], Nazarenko O.B.[1*], Derina K.V.[1], Galtseva O.V.[1, 2]

[1]Tomsk Polytechnic University, Tomsk, Russia
[2] Tomsk State University of Control Systems and Radioelectronics, Tomsk, Russia
*Corresponding author: olganaz@tpu.ru

Abstract. *Hydroxyapatite has a wide range of possible applications in biomedicine, optics and electronics, sensors, catalysis and in environmental decontamination. The present study focused on the synthesis of hydroxyapatite by the wet precipitation method. The influence of drying time on the properties of synthesized material was investigated. The particle size increases from 80 to 200 μm by increasing the drying time from 24 hours to 96 hours. The morphology and properties of hydroxyapatite powders obtained under the action of the ultraviolet radiation and ultrasonic exposure acting together and individually was studied. The obtained samples were analyzed using X-ray diffraction, Fourier transform infrared spectroscopy, scanning electron microscope, Brunauer–Emmett–Teller methods. The results showed that the properties of the obtained hydroxyapatite powders were highly dependent on the synthesis conditions. Ultrasonic treatment at the synthesis stage led to a decrease in the size of the resulting hydroxyapatite particles to 4 μm. The use of ultraviolet radiation at the stabilization stage led to an increase in the content of hydroxyapatite in the reaction products.*

Keywords: hydroxyapatite, wet precipitation, ultrasound, ultraviolet radiation.

1. Introduction

Hydroxyapatite (HAp) is a calcium phosphate mineral of composition $Ca_{10}(PO_4)_6(OH)_2$, it is widely known as a biomaterial and used for bone repair and bone regeneration [1–3]. HAP has excellent biocompatibility and exhibits dielectric and piezoelectric properties [4]. Theoretically, the band gap of HAP can reach 7.4–7.9 eV, although the values of 3.8–4.5 were observed in the experiments [5,6]. Such values of the band gap make it possible to use HAp as a dielectric in metal-insulator-semiconductor (MIS) structures, which presents new opportunities for sensorics and microelectronics. Based on the fact that HAp has a piezoelectric effect, it is possible to convert some physical influences, such as sound vibrations, touch, temperature, into an electrical signal. This effect is already being used in such devices as sensors, actuator devices, transducers, micro power generators in electronics, civil infrastructure systems, biomedical and automotive applications [7,8]. A number of studies are devoted to the use of HAp in catalytic process: for catalytic oxidation of organic pollutants and CO [9,10], catalytic reduction of CO_2 and N_2O [11,12], for environmental remediation [13].

There are a large number of different methods for the synthesis of HAp. Depending on the composition of the initial substances and the synthesis conditions, the following main methods for obtaining hydroxyapatite can be distinguished: solid state reactions [14], chemical precipitation [15], hydrothermal

synthesis and sol-gel process [16]. In addition, microwave irradiation accelerates the synthesis of HAp and produces a high-purity powder with a small and narrow particle size distribution [17, 18].

Various methods of obtaining hydroxyapatite have their advantages and disadvantages due to the multifactorial nature of the synthesis process, the need to coordinate such parameters as reaction temperature, pH, molar ratio of chemicals, etc. to obtain a product with the required properties [19]. Therefore, researchers are studying the possibility of influencing the reaction mixture to various factors, including ultraviolet (UV) radiation and ultrasonic (US) exposure, in order to synthesize HAp with desired characteristics. UV irradiation of the source materials made it possible to carry out the solid-phase synthesis of HAp without the use of heat treatment [20-21]. It was found that ultrasonic treatment of the initial suspension of calcium hydroxide during chemical precipitation increases the rate of formation of the hydroxyapatite nanocrystalline phase [22, 23].

The aim of the present work is to study the effect of drying time, ultraviolet radiation and ultrasonic exposure on the synthesis of hydroxyapatite by the wet precipitation method and the properties of synthesized material.

2. Materials and methods

The starting materials for the synthesis of HAp were calcium hydroxide $Ca(OH)_2$, distilled water, orthophosphoric acid H_3PO_4. Figure 1 shows the scheme for obtaining hydroxyapatite, according to which the process consists of the following stages: preparation of initial solutions – synthesis – stabilization – filtration and washing – drying. In this synthesis method, by controlling the feed rate of the phosphoric acid solution and its concentration, it is possible to ensure complete interaction of the initial reagents, which will exclude the formation of side phosphates or minimize this probability, leading the entire synthesis to the desired result – calcium hydroxyapatite of stoichiometric composition.

8% solution of orthophosphoric acid and 20% suspension of calcium hydroxide were prepared at the first stage. The calcium hydroxide suspension was loaded into the reactor at the second stage. A solution of orthophosphoric acid was added and reacts with calcium hydroxide according to the following reaction with continuous stirring [24, 25]:

$10\ Ca(OH)_2 + 6H_3PO_4 \rightarrow Ca_{10}(PO_4)_6(OH)_2 + 18H_2O$.

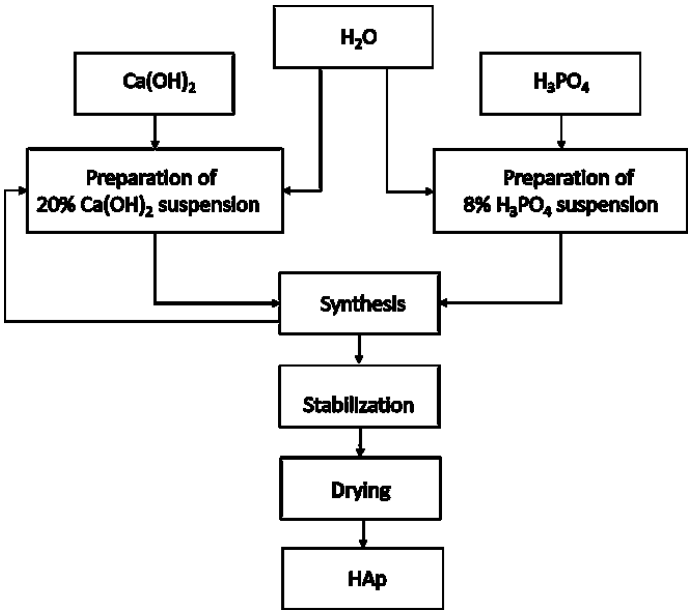

Fig.1. Scheme for synthesis of hydroxyapatite.

Synthesis time varied depending on the quantity of reagents used. It took 65 minutes to produce 20 grams of hydroxyapatite. In order for all reagents to completely react with each other, a stage of stabilization of the hydroxyapatite solution was introduced. This process was carried out at room temperature. Stabilization should be carried out in a sealed container to avoid impurities. The solution was infused for a

day from the moment of stopping stirring. As a result, HAp was at the bottom of the vessel, and the liquid phase was at the top. After the stabilization stage, the obtained sample was washed with distilled water until a neutral medium was obtained, which was controlled by a litmus indicator. Then, the resultant suspension was filtered through the "blue ribbon" filter, as a result of which HAp was separated from the liquid phase. At the stage of drying, HAp was dried at room temperature until the liquid is completely removed. To study the effect of drying time on the structure of the material, drying was carried out for 24 hours and 96 hours. To obtain the final product in the form of a powder, the synthesized material was ground using an agate mortar and pestle.

To study the influence of external factors on the change in the properties of the HAp obtained during the synthesis, ultrasonic (US) exposure, ultraviolet (UV) irradiation separately at various stages of production, as well as their combination, were used. The mixture of reagents in the reactor at the stage of synthesis was exposed to ultrasound at a frequency of 20 kHz for 20 min. At the stabilization stage, the synthesized sample was irradiated with ultraviolet. The wavelength of ultraviolet radiation was 180 nm. The following combinations of the experimental conditions have been investigated:

1) wet precipitation without the stabilization stage (standard conditions according to the methodology);
2) US (20 minutes, synthesis stage) and UV (120 minutes, stabilization stage);
3) US (20 minutes, synthesis stage);
4) UV (120 minutes, stabilization stage);
5) wet precipitation including the stabilization stage.

The phase composition of the obtained samples was analyzed by the X-ray diffraction (XRD) method using a Difray 401 diffractometer (JSC Scientific Instruments, St. Petersburg, Russia). The XRD peaks were recorded in 2Θ range of 30–110°, CuKα, λ = 1.5405 Å. Identification of crystalline phases was achieved by comparing the recorded diffraction patterns with ICDD PDF2 database; numbers of patterns from database, that was 11008 and 30747.

The functional groups of the obtained samples were identified by the method of Fourier transform infrared spectroscopy (FTIR) using a Shimadzu IRPrestige-21 FTIR spectrophotometer (Shimadzu, Kyoto, Japan). The analysis was performed in the absorption mode in the wavelength range from 400 cm^{-1} to 4000 cm^{-1} with a resolution of 4 cm^{-1}. The surface morphology and microstructure of the obtained samples was studied using a scanning electron microscope (SEM) TESCAN VEGA 3 SBU (Brno, Czech Republic) with an OXFORD X-Max 50 energy-dispersive adapter (High Wycombe, UK), operated at 10–20 kV accelerating voltage, specimen current of 3–12 nA, and a spot diameter of ~2 μm.

The surface area study was carried out using the BET adsorption method with the calculation of pore diameter using the BJH method [26]. Measurements were performed using a 3P Sync 420A specific surface area and porosity adsorption analyzer (3P Instruments, Germany). Nitrogen was used as an adsorptive. The results were processed using built-in software. All samples were pre-dried to remove gases for 10 hours at 200 °C. Based on the results of the analysis, adsorption isotherms were obtained.

3. Research results

3.1 Effect of drying time

Using scanning electron microscopy, the morphology of the samples for drying time of 24 and 96 hours was analyzed. The SEM images with different magnification are shown in Figure 2. All synthesized particles are characterized by the form of aggregates and porous structure. With a drying time of 24 hours, the particles have a size of more than 80 μm. With an increase in drying time to 96 hours, the particle size becomes larger than 200 μm, and the faceting becomes more noticeable. Based on the XRD-results shown in Figure 3, it was revealed that both samples correspond to the crystalline phase of calcium hydroxyapatite and do not contain additional reflections of other phases. On the XRD pattern of the Sample 1, there is a doubling high for reflections, which is associated with incomplete crystallization.

3.2 Influence of external factors

FTIR spectra of the samples obtained under the influence of external factors of ultrasonic and ultraviolet exposure and control samples are shown in Figure 4. Absorption bands related to the phosphate group PO_4^{3-} are observed at 470, 567, 603, 962 and 1039÷1080 cm^{-1} [27]. The absorption bands at 873 and 1421÷1465 cm^{-1} is attributed to CO_3^- groups [27, 28], the presence of which can be explained by the

adsorption of atmospheric carbon dioxide during sample preparation. The broad absorption band at 3420 cm^{-1} and weak band at 1640 cm^{-1} are due to the presence of adsorbed water molecules [29].

The bands appearing at 3571 cm^{-1} corresponds to the hydroxyl bond stretch which is characteristic of stoichiometric HAp [27]. Comparing the spectra with each other, we can conclude that US exposure (Sample 3) and the combined action of US and UV (Sample 2) does not give particularly noticeable changes. At the same time, in the case of using only UV radiation (Sample 4), it can be seen that UV radiation has a weak effect on water, but actively destroys carbon compounds.

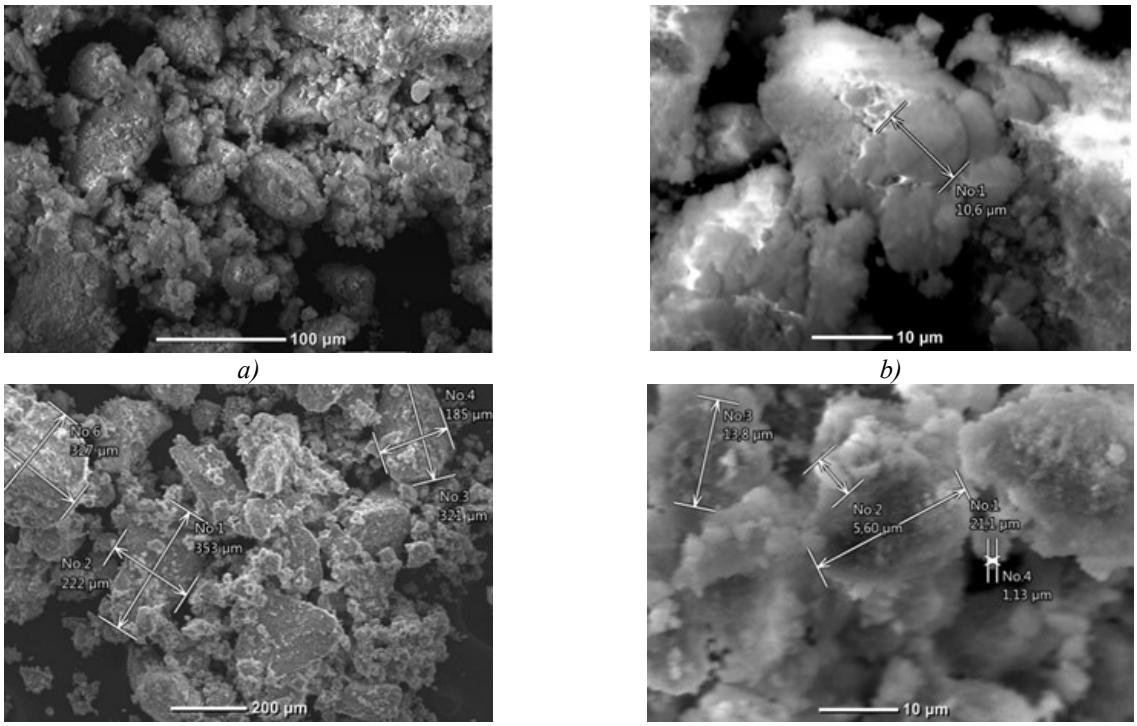

a) *b)* *c)* *d)*

Fig.2. SEM images of the HAp samples obtained at different drying time: 24 h (a, b) and 96 h (c, d).

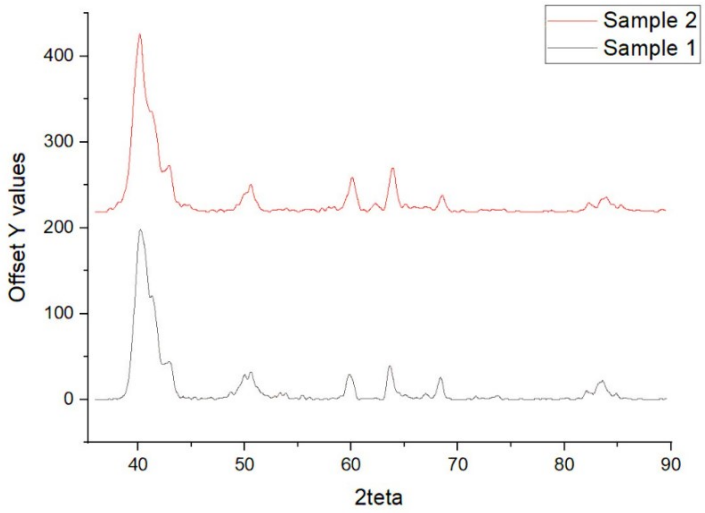

Fig.3. XRD patterns of the HAp samples obtained at different drying time: 24 h (Sample 1) and 96 h (Sample 2).

Figure 5 shows the XRD patterns of the HAp samples obtained under the influence of US exposure and UV radiation and of the control samples. According to the XRD data, the highest content of HAp is characteristic of the sample obtained by exposure to UV radiation only (Sample 4). The lowest content of hydroxyapatite is typical for the Sample 1, where the wet precipitation method without stabilization stage was used.

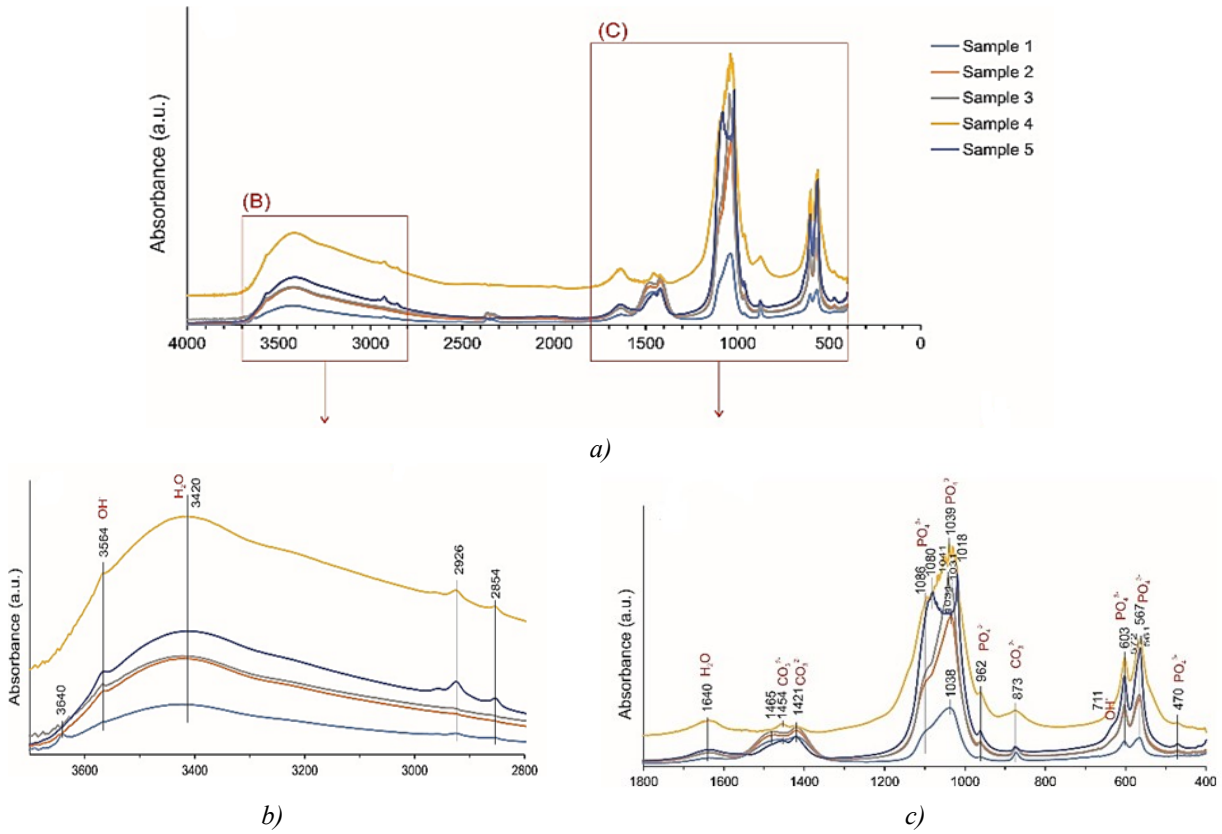

Fig.4. FTIR spectra of the HAp samples obtained under the influence of external factors.

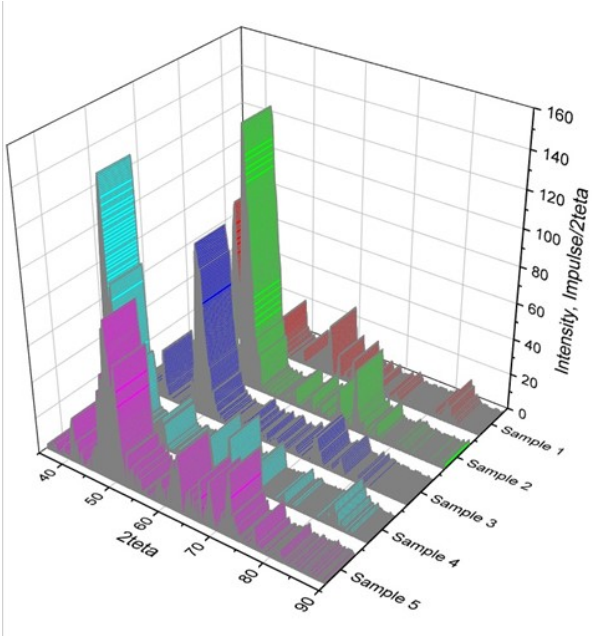

Fig.5. XRD patterns of the HAp samples obtained under the influence of external factors.

Figure 6 and 7 show the SEM images of the control samples synthesized under conditions without external influences and the samples under the action of US and UV. The Sample 1 is characterized by the presence of a greater number of agglomerates with a size of more than 100 μm, compared with Sample 5, for which the particle size is from 100 μm to 15 μm or less (Figure 6). Thus, introduction of the stabilization stage makes it possible to obtain the particles of smaller sizes without additional use of external factors. The Sample 2 (US+UV) and Sample 3 (US) are characterized by a rounded structure, which was formed as a result of a decrease in the crystallization rate due to US exposure (Figure 7).

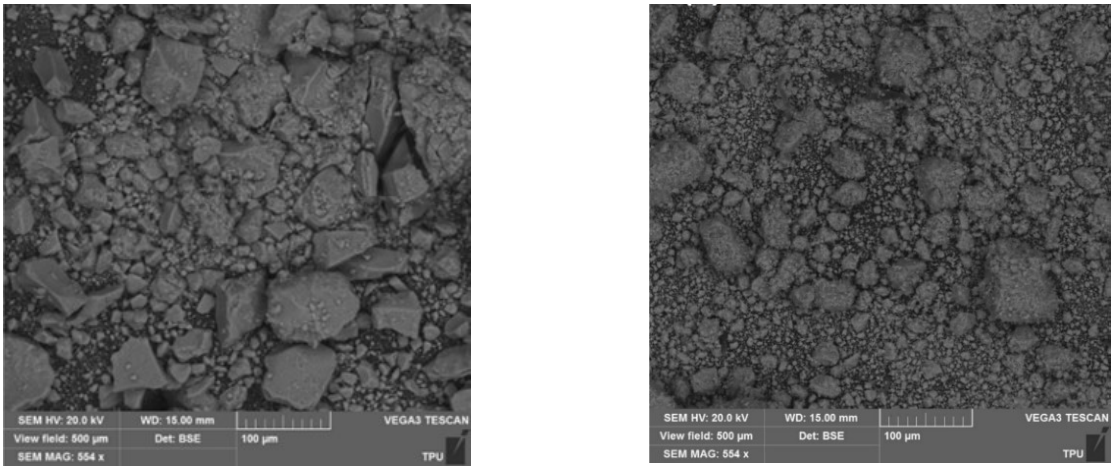

a) *b)*

Fig.6. SEM images of the HAp obtained at standard conditions of wet precipitation: Sample 1 (a), Sample 5 (b).

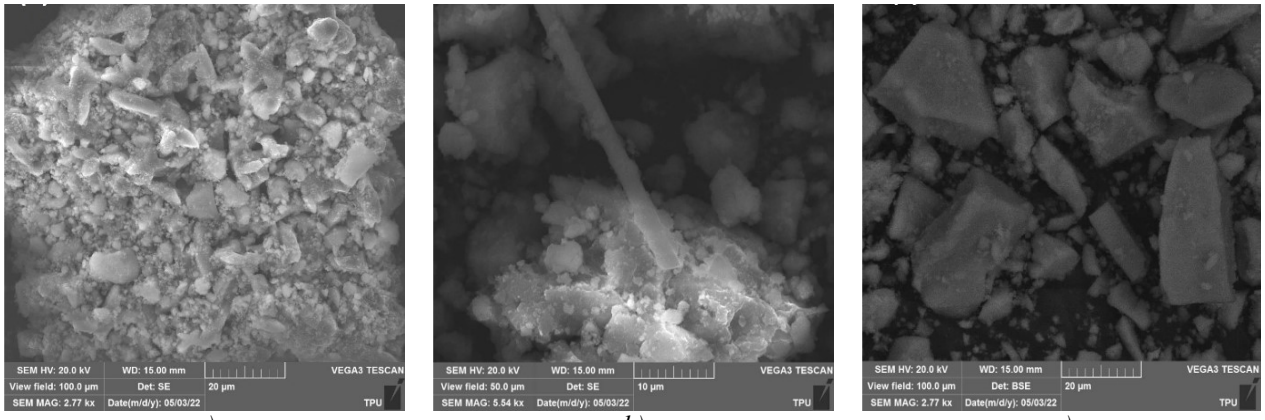

a) *b)* *c)*

Fig.7. SEM images of the HAp obtained under the influence of external factors: Sample 2 (a), Sample 3 (b), Sample 4 (c).

These samples are characterized by particle sizes from 4 µm to 1 µm or less. The Sample 4, obtained under exposure to UV only, is characterized by a faceted structure, which may be due to the fact that the crystallization processes were not interfered with by US. In this case, the particle sizes are in the range from 20 µm to 2 µm or less. The use of ultrasound at the stage of synthesis prevents the formation of bonds between particles and makes it possible to significantly reduce the size of the obtained particles with a spherical shape, in contrast to faceted crystallites in the case of ultraviolet irradiation.

Adsorption isotherms with sorption hysteresis were obtained, which are typical for systems with weak interaction of the adsorbate with the adsorbent, based on the results of the analysis of the specific surface area. The results are summarized in Table 1. It follows that the considered external influences on the synthesis of HAp increase the average pore diameter from the analysis of the data obtained, while a significant decrease in the specific surface area occurs, except for Sample 3. Thus, short-term exposure to ultrasound on a sample of hydroxyapatite during its synthesis leads to an increase in the specific surface area surface and the increase in average pore size.

Table 1. Specific surface area and pore size of the HAp samples obtained under the influence of external factors.

Parameters	Sample number				
	1	2	3	4	5
BET surface area (m^2/g)	138.280	118.239	157.628	110.235	117.492
Average pore diameter (nm)	9.450	12.076	13.445	15.367	10.390

4. Conclusion

In this study, hydroxyapatite was obtained by wet precipitation method. A stabilization stage was introduced into the technological scheme of synthesis, due to which the average particle size of the obtained hydroxyapatite was reduced to 15 μm. The drying time of the obtained hydroxyapatite affects the particle size of the material. An increase in the duration of drying of hydroxyapatite from 24 to 96 hours led to an increase in particle size up from 80 μm to 200 μm and to a more pronounced faceting. It was found that the use of ultraviolet irradiation at the stabilization stage makes it possible to increase the content of the main product – hydroxyapatite of stoichiometric composition. The ultrasonic treatment of reagents at the stage of HAp synthesis for 20 min led to a reduction in the size of the obtained HAp particles with a spherical shape from 15 μm to 4 μm. In addition, the production of hydroxyapatite under ultrasound exposure resulted in an increase in the specific surface area of particles by 14% and the average pore size by 42% compared to the wet precipitation method under standard conditions. The method of hydroxyapatite production considered in this work allows synthesizing a bulk material, unlike the CVD or PVD methods traditionally used to produce hydroxyapatite-based coatings [30]. Using the proposed method will allow to create bulk medical products filled with hydroxyapatite with the required properties.

Conflict of interest statement

The authors declare that they have no conflict of interest in relation to this research, whether financial, personal, authorship or otherwise, that could affect the research and its results presented in this paper.

CRediT author statement

Mostovshchikov A.V.: Writing – original draft, Methodology, Conceptualization; Grebnev M.E.: Investigation, Visualization; Rudmin M.A.: Formal analysis, Data curation; Nazarenko O.B.: Writing – review & editing, Validation, Supervision; Derina K.V.: Investigation; Galtseva O.V.: Formal analysis.

The final manuscript was read and approved by all authors.

Acknowledgments

This research was supported by the Tomsk Polytechnic University development program.

The equipment of the TPU's "Physical and chemical methods of analysis" has been applied.

References

1 LeGeros R.Z., LeGeros J.P. Hydroxyapatite. (2008) *Bioceramics and their Clinical Applications*. Woodhead Publishing. 367 – 394. DOI: 10.1533/9781845694227.2.367.

2 Rial R., González-Durruthy M., Liu Z., Ruso J.M. (2021) Advanced materials based on nanosized hydroxyapatite. *Molecules*, 26, 3190. DOI: 10.3390/molecules26113190.

3 Dorozhkin S.V. (2022) Calcium orthophosphate (CaPO4)-based bioceramics: preparation, properties, and applications. *Coating,* 12, 1380. DOI: 10.3390/coatings12101380.

4 Das A., Pamu D. (2019) A comprehensive review on electrical properties of hydroxyapatite based ceramic composites. *Materials Science and Engineering: C,* 101, 539–563. DOI: 10.1016/j.msec.2019.03.077.

5 Corno M., Busco C., Civalleri B., Ugliengo P. (2006) Periodic ab initio study of structural and vibrational features of hexagonal hydroxyapatite $Ca_{10}(PO_4)_6(OH)_2$. *Physical Chemistry Chemical Physics,* 8, 2464–2472. DOI:10.1039/B602419J.

6 Bystrov V., Paramonova E., Avakyan L., Coutinho J., Bulina N. (2021) Simulation and computer study of structures and physical properties of hydroxyapatite with various defects. *Nanomaterials,* 11, 2752. DOI:10.3390/nano11102752.

7 Yang Z., Zhou S., Zu J., Inman D. (2018) High-performance piezoelectric energy harvesters and their applications. *Joule,* 2(4), 642–697. DOI:10.1016/j.joule.2018.03.011.

8 Aabid A., Raheman M.A., Ibrahim Y.E., et al. (2021) A systematic review of piezoelectric materials and energy harvesters for industrial applications. *Sensors,* 21, 4145. DOI: 10.3390/s21124145.

9 Xu Z., Li C., Wang N., Ding Y., Yan Z., Li Q. (2024) Functional graphitic carbon nitride/hydroxyapatite heterojunction for robust formaldehyde removal at ambient temperature. *Journal of Environmental Chemical Engineering,* 12(1), 111679. DOI: 10.1016/j.jece.2023.111679.

10 Lan Y.-T., Yang X.-Y., Liu S.-X., Miao Y.-X., Zhao Z. (2022) Highly dispersed silver nanoparticles supported on a hydroxyapatite catalyst with different morphologies for CO oxidation. *New Journal of Chemistry,* 46, 6940–6945. DOI: 10.1039/D2NJ00464J.

11 Wang Y., Zhou X., Wei X., et al. (2021) Co/hydroxyapatite catalysts for N_2O catalytic decomposition: design of well-defined active sites with geometrical and spacing effects. *Molecular Catalysis*, 501, 111370. DOI:10.1016/j.mcat.2020.111370.

12 Guo J., Duchesne P.N., Wang L., et al. (2020) High-performance, scalable, and low-cost copper hydroxyapatite for photothermal CO_2 reduction. *ACS Catalysis,* 10, 13668–13681. DOI: 10.1021/acscatal.0c03806.

13 Yamada H., Tamura K., Watanabe Y., Iyi N., Morimoto K. (2011) Geomaterials: their application to environmental remediation. *Science and Technology of Advanced Materials,* 12, 064705. DOI: 10.1088/1468-6996/12/6/064705.

14 Javadinejad H.R., Ebrahimi-Kahrizsangi R. (2021) Thermal and kinetic study of hydroxyapatite formation by solid-state reaction. *International Journal of Chemical Kinetics*, 53, 583–595. DOI: 10.1002/kin.21467.

15 Mobasherpour I., Soulati Heshajin M., Kazemzadeh A., Zakeri M. (2007) Synthesis of nanocrystalline hydroxyapatite by using precipitation method. *Journal of Alloys and Compounds*, 430, 330–333. DOI:10.1016/j.jallcom.2006.05.018.

16 Bilton M., Milne S.J., Brown A.P. (2012) Comparison of hydrothermal and sol-gel synthesis of nano-particulate hydroxyapatite by characterization at the bulk and particle level. *Open Journal of Inorganic Non-metallic Materials*, 2, 1–10. DOI: 10.4236/ojinm.2012.21001.

17 Yang Y., Ong J.L., Tian J. (2002) Rapid sintering of hydroxyapatite by microwave processing. *Journal of Materials Science Letters*, 21, 67–69. DOI: 10.1023/A:1014250813564.

18 Shaban N.Z., Kenawy M.Y., Taha N.A., Abd El-Latif M.M., Ghareeb D.A. (2021) Synthesized nanorods hydroxyapatite by microwave-assisted technology for in vitro osteoporotic bone regeneration through Wnt/β-catenin pathway. *Materials*, 14, 5823. DOI: 10.3390/ma14195823.

19 Mohd Pu'ad N.A.S., Abdul Haq R.H., Mohd Noh H., Abdullah H.Z., Idris M.I., Lee T.C. (2020) Synthesis method of hydroxyapatite: a review. *Materials Today: Proceedings,* 29(1), 233–239. DOI:10.1016/j.matpr.2020.05.536.

20 Sultana S., Hossain M.S., Mahmud M., et al. (2021) UV-assisted synthesis of hydroxyapatite from eggshells at ambient temperature: cytotoxicity, drug delivery and bioactivity. *RSC Advances*, 11(6), 3686–3694. DOI:10.1039/D0RA09673C.

21 Leonov A., Usacheva T., Lyapunov D., Voronina N., Galtseva O., Rogachev A. (2021) Improving the heat resistance of polymer electrical insulation systems for the modernization of induction motors. *Eurasian Physical Technical Journal*, 18(1) (35), 34–42. DOI: 10.31489/2021No1/34-42.

22 Poinern G.E., Brundavanam R.K., Mondinos N., Jiang Z.T. (2009) Synthesis and characterisation of nanohydroxyapatite using an ultrasound assisted method. *Ultrasonics Sonochemistry*, 16(4), 469–474. DOI:10.1016/j.ultsonch.2009.01.007.

23 Rouhani P., Taghavinia N., Rouhani S. (2010) Rapid growth of hydroxyapatite nanoparticles using ultrasonic irradiation. *Ultrasonics Sonochemistry,* 17(5), 853–856. DOI:10.1016/j.ultsonch.2010.01.010.

24 Bouyer E., Gitzhofer F., Boulos M.I. (2000) Morphological study of hydroxyapatite nanocrystal suspension, *Journal of Materials Science: Materials in Medicine*, 11(8), 523–531. DOI: 10.1023/A:1008918110156.

25 Agbeboh N.I., Oladele I.O., Daramola O.O., Adediran A.A., Olasukanmi O.O., Tanimola M.O. (2020) Environmentally sustainable processes for the synthesis of hydroxyapatite. *Heliyon*, 6(4), e03765. DOI:10.1016/j.heliyon.2020.e03765.

26 Sing K.S.W. (1998) Adsorption methods for the characterization of porous materials. *Advances in Colloid and Interface Science,* 76–77, 3–11. DOI:10.1016/S0001-8686(98)00038-4.

27 Kannan S., Lemos A.F., Ferreira J.M.F. (2006) Synthesis and mechanical performance of biological-like hydroxyapatites. *Chemistry of Materials*, 18(8), 2181–2186. DOI:10.1021/cm052567q.

28 Szterner P., Biernat M. (2022) The synthesis of hydroxyapatite by hydrothermal process with calcium lactate pentahydrate: the effect of reagent concentrations, pH, temperature, and pressure. *Bioinorganic Chemistry and Applications,* 3481677. DOI: 10.1155/2022/3481677.

29 Wang Y.J., Chen J.D., Wei K., Zhang S.H., Wang X.D. (2006) Surfactant-assisted synthesis of hydroxyapatite particles. *Materials Letters*, 60(27), 3227–3231. DOI: 10.1016/j.matlet.2006.02.077.

30 Safavi M.S., Walsh F.C., Surmeneva M.A., Surmenev R.A., Khalil-Allafi J. (2021) Electrodeposited hydroxyapatite-based biocoatings: Recent progress and future challenges. *Coatings*, 11, 110. DOI:10.3390/coatings11010110.

AUTHORS' INFORMATION

Mostovshchikov, Andrei Vladimirovich – Doctor of Technical Sciences, Associate Professor, Professor, School of Earth Sciences and Engineering, Tomsk Polytechnic University; Professor, Department of Physical Electronics, Tomsk State University of Control Systems and Radioelectronics, Tomsk, Russia; Scopus Author ID: 15019762000; ORCID ID: 0000-0001-6401-9243; avmost@tpu.ru

Grebnev, Mark Ernestovich – Master's Student, School of Nuclear Science & Engineering, Tomsk State University of Control Systems and Radioelectronics, Tomsk, Russia; ORCID ID: 0009-0003-0937-5298; mark18091@gmail.com
Rudmin, Maxim Andreevich – Candidate of Geological and Mineralogical Sciences, Associate Professor, Division for Geology, School of Earth Sciences and Engineering, Tomsk polytechnic university, Tomsk, Russia; Scopus Author ID: 56350797200**;** ORCID ID: 0000-0002-9004-9929**;** rudminma@tpu.ru
Nazarenko, Olga Bronislavovna – Doctor of Technical Sciences, Professor, Division of Testing and Diagnostics, NDT School, Tomsk polytechnic university, Tomsk, Russia; Scopus Author ID: 57193908313; ORCID ID: 0000-0003-3245-3584; olganaz@tpu.ru
Derina, Ksenia Vladimirovna – Candidate of Technical Sciences, Associate Professor, Division of Chemical Engineering, School of Earth Sciences and Engineering, Tomsk Polytechnic University, Tomsk, Russia; Scopus Author ID: 57195258640; ORCID ID: 0000-0003-1663-4019; derinakv@tpu.ru
Galtseva, Olga Valerievna – Candidate of Technical Sciences, Associate Professor, Division of Testing and Diagnostics, NDT School, Tomsk Polytechnic University; Associate Professor, Department of Innovation Management, Tomsk State University of Control Systems and Radioelectronics, Tomsk, Russia; Scopus Author ID: 15049236900; ORCID ID: 0000-0001-6919-4833; tpuolga@tpu.ru